Chapter one

Introduction

1.1 General approach

Ferrites are chemical compounds which are composed of a ceramic material and iron oxide as main component [1]. Spinel ferrites are represented by the formula unit AB_2O_4. Most of the spinel ferrites form cubic spinel structure with oxygen anions in face center cubic (fcc) positions and cations in the tetrahedral and octahedral coordinated interstitial lattice sites, forming the A and B sublattices [2]. Depending upon the nature (magnetic or non-magnetic) and distribution of cations among A and B sublattices, spinel ferrites can exhibit properties of different type magnets, such as ferrimagnet, antiferromagnet and paramagnet [3]. Soft ferrites are the most widely used magnetic materials for low-cost, high-performance, and high-frequency applications. Ferrites are stable and easily manufactured and possess environmental stability [4]. The usefulness of ferrite is influenced by the physical and chemical properties of the materials and depends on many factors including the preparation conditions, such as sintering temperature, sintering time, heating and cooling rates, and grinding time [5]. The hard ferrites have gained a great significance in the technology during the last decades. New applications were found for these ceramic permanent magnets. In most small dc-motors the wire wound field was replaced by the

permanent field of hard ferrites, but the permanent magnets had to meet special requirements and this means that they must have special properties. The variations or tolerances of these magnetic properties were limited partially very narrowly. Therefore, it is necessary to know the correlation between manufacturing parameters and the magnetic properties [6].

Glass ceramics containing ferromagnetic, ferromagnetic or super paramagnetic particles have potentially useful applications in different fields of electronic products [7]. Several investigators have focused their attention on Ni-Cu ferrite because copper containing ferrites have interesting magnetic and electrical properties [8,9]. Ni-Cu ferrites are preferred because of improved magnetic properties, high frequency response and high resistance. In the field of electronics, researchers continue to investigate the design of superstructures comprised of magnetically ordered arrays to enhance the sensitivity in magnetic sensors. The stability of electronic and high density data storage devices made by magnetic nano-composites is limited by their super paramagnetic transition. Thus, while current efforts are aimed at increasing the thermal energy barrier against the magnetic reversal in magnetic nanocomposites, there is strong interest to understand the magnetization processes in the super paramagnetic region [10].

1.1.1 Magnetite

The term *ferrite* is commonly used generically to describe a class of magnetic oxide compounds that contain iron oxide as a principal component. Magnetite (Fe_3O_4), also called *loadstone*, is a genuine ferrite and was the first

magnetic material known to the ancient people. Ferrites are a unique class of compounds comprising lanthanides and fast transition metals in particular, iron, chromium, and manganese. The general formula is $M^{II}M_2O_4$, where M^{II} is a divalent metal ion such as Fe^{2+}, Mg^{2+}, Ni^{2+}, Co^{2+}, Zn^{2+}, Cu^{2+} and M is a trivalent metal ion such as Fe^{3+}, Cr^{3+}, Al^{3+}, Mn^{3+} [11].

1.1.2 Cobalt ferrite

Cobalt ferrite is categorized into a hard magnet due to its high corecivity and moderate magnetization. Due to its high magnetic corecivity value and good physical and chemical stability it has been used for various applications. Cobalt ferrite neither has a spinel or inverse spinel structure, it has partially inverse spinel structure $[(Co_k{}^{2+}Fe_{1-k}{}^{3+})(Co_{1-k}{}^{2+}Fe_{1-k}{}^{3+})O_4]$. The cation distribution can be distinctly characterized by the so-called degree of inversion (k) in normal spinels (k=0), while in the inverse spinel (k=1), Cobalt ferrite become a perfect for using in high density magnetic storage materials, medical diagnosis, magneto-mechanical, and torque sensors [12].

1.1.3 Manganese ferrite

Manganese ferrite ($MnFe_2O_4$) nano-particles have been of great interest for their remarkable soft-magnetic properties (low coercivity, moderate saturation magnetization) accompanied by good chemical stability and mechanical hardness [13]. Recently, they received increased attention for their application as a negative contrast agents (CAs) in magnetic resonance imaging (MRI) [14,15]. Indeed super paramagnetic $MnFe_2O_4$ nano-particles

were found very useful in MRI for the detection of tumors and definition of damaged zones in local edemas or hemorrhages [16].

1.1.4 Nickel ferrite

Nickel ferrite ($NiFe_2O_4$) nano-particles have been widely studied for their unique magnetic properties which can be influenced by their shape, particle size and their composites with other material [17-19]. Nickel ferrite based nano-materials also have different practical applications in high frequency devices, power transformers, drug delivery and gas sensors [20].

1.1.5 Copper ferrite

The copper ferrite has two crystallographic spinel structures, the high temperature cubic phase and low temperature tetragonal phase. Since Cu^{2+} is a Jahn-Teller ion, it gives the anomalous favorable properties and also exhibits phase transition from tetragonal to cubic, depending on the temperature. $CuFe_2O_4$ can be describe as cubic close-packed arrangement of oxygen ions, with Cu^{2+} and Fe^{3+} ions at two different crystallographic sites. From structure standpoint, the formula unit of stoichiometric ferrite can be written as: $(Cu_{\delta}Fe_{1-\delta})$ $A[Cu_{1-\delta}\ Fe_{1+\delta}]BO_4$,where A denotes for tetrahedral sites, B represents octahedral sites, the parameter of inversion δ is equal to 0 for inverse spinel ,and to 1,when the spinel is normal. The Cu-Fe-O system has been long standing interest in solid-state physics, mineralogy, ceramics and metallurgy [21].

1.2 Magnetic materials

Material science and engineering play an imperative role in this modern age of science and technology. The drastic progress in the development and growth of electronic ceramics since the era of post Second World War II has played a major role in the transformation of the society from steel age to the information age. Nearly instantaneous satellite communications from coast to coast and around the world would not be possible without simultaneous advances in semiconductors, dielectrics, ferroelectrics, ferrites and optoelectronics. The continued developments in these fields have been matched, and perhaps eventually superseded with advances in superconducting ceramics, photonics, and optical waveguides and potentially in optical computing and information processing [22].

In connection with advances in communication technologies, magnetic ceramics have been investigated due to their vastly intriguing properties such as magnetization behaviour, high magnetic permeability and high electrical resistivity [23]. These intrinsic material properties have made them indispensably the most versatile engineering ceramics for high frequency applications including power transformers, antennas, faraday rotators, etc [24].

A magnetization (M) can occur as a result of more or less alignment of elementary magnets known as magnetic dipole (electron orbits or electron spins) present in a matter. In order to produce this alignment of magnetic dipole, an external magnetic field (H) is to be applied. When magnetization is relatively small, it increases proportionally with an applied field according to

the relation, $M = \chi H$, where χ is the susceptibility per cm^3 [25]. Magnetism in the material can be classified in terms of the arrangements of magnetic dipoles in the solid and depending upon the sign and the value of susceptibility (χ). These dipoles can be thought of, a little imprecisely, as microscopic bar magnets attached to the various atoms present.

1.3 Classification of ferrites

Ferrites are a very well established group of magnetic semiconductor materials. Ferrites are classified by the following categories.

1.3.1 On the basis of crystal structure

On the basis of their crystal structure ferrites are of three types namely Hexagonal ferrite, Garnet and Spinel ferrite [26]. By virtue of their crystal structure they can accommodate variety if cations at available sites enabling wide variation in electrical and magnetic properties.

1.3.1.1 Hexagonal ferrite

In 1952, a new class of ferrites having permanent magnetic properties was discovered. Workers at Philips laboratory at Eindhoven in the Netherlands made the developments of hexagonal ferrites possible. Hexagonal ferrites (general formula $MFe_{12}O_{19}$ where M is usually Barium Ba, Strontium Sr, Calcium Ca or Lead Pb) have been distinguished due to their high uniaxial magnetocrystalline anisotropy which renders them perfect for permanent (hard) magnet applications [27]. The crystal structure of

hexaferrite is complex but it can be described as hexagonal with a unique c axis, which is the easy axis of magnetization in the basic structure.

1.3.1.2 Garnet

The second group of ferrites is the garnet type ferrites. Garnets, unique magnetic ceramics have optical transparency and used in magneto-optical applications [28]. Yttrium iron garnet (YIG) is a synthetic garnet with chemical composition Y3Fe5O12. Yttrium can be replaced by one of the rare earth ions like La^{3+}, Dy^{3+}, Gd^{3+}, Er^{3+}, etc. with an atomic number greater than 61.

1.3.1.3 Spinel ferrite

Spinel ferrite having the generic formula MFe_2O_4 in which M and Fe display tetrahedral and octahedral cation sites, respectively, and O indicates the oxygen anion site. They are also called cubic ferrites. In spinel ferrites, the relatively large oxygen anions form a cubic close packing with ½ of the octahedral and ⅛ of the tetrahedral interstitial sites occupied by metal ions. Spinel ferrites with the formula $MOFe_2O_3$ or where M^{II} represents a divalent metal cation such as Mn, Fe, Co, Ni, Cu, Zn, Cd, Mg, and Fe^{III} is the trivalent iron cation, have the same crystallographic structure as the mineral spinel ($MgAl_2O_4$), [29,30].

1.3.1.4 Random spinel

The divalent metal ions M^{2+} and trivalent Fe^{3+} ions in ferrite the spinel formula AB_2O_4 are distributed at both tetrahedral A site and octahedral B site,

in this case then the ferrite is termed as random spinel ferrite. It has an intermediate cation distribution, represented as $[Fe_{0.67}\ M_{0.33}]_{tet}\ [M_{0.67}\ Fe_{1.33}]_{oct}O_4$. It has been established now that in the elementary unit cell of spinel structure eight tetrahedral and sixteen octahedral sites are occupied by metal ions and completely normal and inverse spinel represent the extreme cases. The distribution of ions between two types of sites is determined by a delicate balance contribution, such as the magnitude of ionic radii, their electronic configuration and the electrostatic energy of the lattice. The best known example of random spinel ferrite is copper ferrite [31].

1.3.1.5 Normal spinel

A material with the normal spinel structure having general formula $M(Fe_2)O_4$ has all the divalent metal (M) cations on the tetrahedral (A) sites and the trivalent (Fe) cations on the octahedral [B] sites [32]. This can be represented by the formula $[M]_{tet}\ [Fe_2]_{oct}\ O_4$. Examples of normal spinel are illustrated in Table 1.1.

Table 1.1: The normal spinel ferrite [32]

$MgO.Al_2O_3$	$= MgAl_2O_4$	(normal, parent
$ZnO.Fe_2O_3$	$= ZnFe_2O_4$	mineral) (normal)
$FeO.Al_2O_3$	$= FeAl_2O_4$	(normal)
$CoO.Al_2O_3$	$= CoAl_2O_4$	(normal)
$MnO.Al_2O_3$	$= MnAl_2O_4$	(normal)
$NiO.Al_2O_3$	$= NiAl_2O_4$	(normal

1.3.1.6 Inverse spinel

The normal spinel structure of ferrite is MFe_2O_4, in an inverse spinel structure, Fe(M Fe) O_4, the divalent cations has stronger affinity for an octahedral [B] sites and the trivalent cations are equally divided among the (A) and remaining [B] sites. This can be represented by formula, $[Fe]_{tet}$ [M, $Fe]_{oct}O_4$. For example cobalt ferrite ($CoFe_2O_4$) is predominantly an inverse spinel with a formula; $CoxFe_{1-x}$ (Co_{1-x} Fe_{1+x}) O_4 (with x = 0) where, x is the cation distribution factor which describes the fraction of tetrahedral sites occupied by Co^{2+}cations.

Table 1.2 The Inverse spinel ferrite [33]

$CoO.Fe_2O_3$ $NiO.Fe_2O_3$ $MgO.Fe_2O_3$	$=FeCoFeO_4$ $= FeNiFeO_4$ $=FeMgFeO_4$	(inverse) (inverse) (inverse)

1.3.2 On The Basis of Magnetism

Due to the persistence of their magnetization, the ferrites are of two types i.e. hard and soft. This classification is based on their ability to be magnetized or demagnetized not their ability to withstand penetration or abrasion. Hard ferrites are difficult to magnetize or demagnetize whereas soft ferrites are easily magnetized or demagnetized [33].

1.3.2.1 Hard ferrites

Hard ferrites are difficult to magnetize or demagnetize. They are used as permanent magnets. Hard ferrites has high coercivity and high remanence after magnetization, the high coercivity means the materials are very resistant to becoming demagnetized, an essential characteristic for a permanent magnet.

The most commonly used hard ferrite is Cobalt ferrite, $CoFe_2O_4$ ($CoO{\cdot}Fe_2O_3$), it is used in magnetic recording applications such as audio-/video-tape and high-density digital recording disks [34].

1.3.2.2 Soft ferrites

Soft Ferrites are those that can be easily magnetized or demagnetized. This shows that soft magnetic materials have low coercive field and high magnetization that is required in many applications.

Table 1.3 Soft magnetic materials and their applications [33]

Frequency	**Materials**	**Applications**
Static < 1 Hz	Soft iron, Fe–Co (permendur) Ni–Fe (permalloy)	Electromagnets, relays
Low frequency 1 Hz–1 kHz	Si steel, permalloy, finmet, magnetic glasses	Transformers, motors, generators
Audio-frequency 100 Hz–100 kHz	Permalloy foils, finmet, magnetic glasses, Fe–Si–Al powder (sendust) Mn–Zn ferrite	Inductors, transformers for Switched mode power supplies, TV fly-back transformers
Radio-frequency 0.1–1000 MHz Microwave >1 GHz	Mn–Zn ferrite, Ni–Zn ferrite	Microwave isolators, circulators,

YIG, Li ferrite		

The hysteresis loop for a soft ferrite should be thin and long, therefore the energy loss is very low in soft magnetic material. Examples are nickel, iron, cobalt, manganese etc. They are used in transformer cores, inductors, recording heads and microwave devices [35]. Soft ferrites have certain advantages over other electromagnetic materials including high resistivity and low eddy current losses over wide range of frequencies. They have high permeability and are stable over a wide range of temperature. These advantages make soft ferrites paramount over all other magnetic materials. Table 1.3 gives the information of soft magnetic materials and its applications in microwave to radio frequency [36].

1.4 Magnetic Behavior

An atom is said to be magnetic if it carries a permanent magnetic moment, usually represented by a vector of constant modulus. Every substance is formed from an assembly of atoms which can be either nonmagnetic or magnetic; in this later case, the direction, and sometime the modulus of the magnetic moment can depend on the particular environment of each atom (nature and position of the neighboring atoms, temperature, applied magnetic field).The genesis of magnetism has to do with the orbital and spin motions of electrons and how the electrons interact with one another as pertained to their spin.

The classification of magnetic materials is based on how they respond to magnetic fields. Although as surprising as it may sound, all matter is magnetic to varying degrees. The main delineating factor is that in some materials there is no collective long range interaction between atomic magnetic moments, whereas in other materials there is a very strong interaction. The main types of magnetism are the following [37].

Diamagnetism, paramagentism, anti-ferromagnetism, ferromagnetism and ferrimagnetisms

1.4.1 Diamagnetism

Diamagnetism is a very weak form of magnetism, and it persists only while an external field is being applied to the material. Although the orbit and spin magnetic moments in such a materials cancel in the absence of external magnetic field, an applied field causes the spin moment to slightly exceed the orbital moment. The magnitude of the induced magnetic moment is extremely small, and in the opposite direction of the applied magnetic field. The relative permeability is less than unity, and the magnetic susceptibility is negative; that is, the magnitude of flux density, B, within a diamagnetic solid is less than a vacuum [37].

1.4.2 Para magnetism

For some other materials such as aluminum, and titanium, each atom possesses a permanent dipole moment due to incomplete cancellation of electron spin and/or orbital magnetic moments, resulting in a net magnetic

moment for the atom even with no applied magnetic field. In the absence of the applied field, the orientation of these atomic magnetic moments is random, but when an external magnetic field is applied, they experience a torque which tends to align them with the direction of the field [37].

1.4.3 Ferromagnetism

In ferromagnetic substances, parallel arrangement of magnetic moments in neighboring atoms. They have high magnetic permeability, capable to become highly magnetic and have the ability to retain a permanent magnetic moment in the absence of an external field. Ferromagnetic materials such as iron, nickel, cobalt and some of the rare earth elements are considered to be the most important magnetic substances [37].

1.4.4 Ferrimagnetisms

The word ferrimagnetisms was first coined by Neel to describe the properties of those substances which below a certain temperature exhibit spontaneous magnetization arising from non-parallel alignment of atomic moments. In ferromagnetic substances, the magnetic moments are not equal and aligned opposite to each other so that there is a net magnetic moment (not equal to zero) such a material is said to be ferromagnetic [37].

1.4.5 Anti-ferromagnetism

Materials that exhibit anti-ferromagnetism, the magnetic moments of atoms or molecules, usually related to the spins of electrons, align in a

regular pattern with neighboring spins(on different sub-lattices) pointing in opposite directions. Anti-ferromagnetism, macroscopically similar to paramagnetism, is a weak form of magnetism. Generally, anti ferromagnetic order may exist at sufficiently low temperatures, vanishing at and above a certain temperature, the Neel temperature (Neel temperature is the temperature at which an anti ferromagnetic material becomes paramagnetic; hence losing its magnetic properties). Above the Neel temperature, the material is typically paramagnetic [38].

Table 1.4 Different types of magnetic behaviors [38]

Types	**Magnetic behavior**	**Magnetic susceptibility**	**Examples**
Diamagnetic	No Magnetic moment	Small and negative	Copper, silver, gold and alumina
Paramagnetic		Small and positive	Aluminum, titanium, and alloys of copper
Ferromagnetic		Very large and positive function of applied field, microstructure dependent	Iron, nickel and cobalt
Antiferromagnetic		Small and positive	Manganese chromium, MnO and NiO
Ferrimagnetic		Large and positive, function of applied field, microstructure dependent	Ferrites

1.5 Literature Review

As far as materials preparation is concerned, different wet chemical methods such as citrate precursor, sulphite hydrazinate, oxalate hydrazinate, etc, have been reported by different investigators. The $Ni_{0.6}Zn_{0.4}Fe_2O_4$ samples have been synthesized using $Ni(NO_3)_2$, $Zn(NO_3)_2$ and $Fe(NO_3)_3$ as precursors by dissolving them in distilled water with the required mole proportions. The precipitating reagent was prepared in distilled water with NaOH by taking their appropriate weights depending upon amount of metal nitrates for co-precipitation of ferrite precursor [39]. This has been done as the temperature required to initiate solid-state reaction in oxides is quite high. But solid state reaction at elevated temperatures does not essentially produce nano-particle materials [40]. Moreover, the nano-particles obtained from bulk material by ball milling suffer from different micro-strain defects and do not exhibit enhanced magnetic properties [41, 42]. The ferrites were prepared by this method are found to exhibit better properties than those prepared by ceramic method [43].

The substitution of Zn in cobalt ferrite was conducted using standard ceramic process. The starting materials used in this study were ZnO, CoO and Fe_2O_3 mixed together to form the composition of $Co_{1-x}Zn_xFe_2O_4$ [44].

Precursor methods like, co-precipitation method [45], hydrothermal precipitation process [46], sol-gel synthesis [47], the micro-emulsions approach [48] and single molecular precursor had been often used to synthesize the Mn-Zn ferrite nano-sized materials.

In 2006, Shunli used citrate method to synthesize Mn-Zn ferrites. Nitrates of all the constituent cations (Co^{2+}, Cu^{2+} and Fe^{3+}) were taken in proper stoichiometric proportions as starting materials. Aqueous solutions of these salts were prepared separately by dissolving the salts in minimum amount of de-ionized water and stirred constantly. The solutions were then mixed together. Aqueous solution of citric acid was prepared in adequate quantity and was added to the prepared salt solution. The mixture was then heated at ~80 °C for two hours with continuous stirring. The solutions were allowed to cool to room temperature and finally they were dried at 65 °C in an oven until they turned into brown color fluffy mass. These precursors were annealed at 700 °C for one hour in a muffle furnace. During this process, the precursor thermally decomposed and gave ferrite powders [49].

In 2010, Aurelija used Sol-gel method to synthesize all transition metal ferrite ceramic samples ($YFeO_3$, $Y_3Fe_5O_{12}$, $CoFe_2O_4$, $NiFe_2O_4$, and $ZnFe_2O_4$) by an aqueous glycolate. The gels were prepared using stoichiometric amounts of analytical-grade $Fe(NO_3)_3{\cdot}9H_2O$, Y_2O_3, $Co(CH_3COO)_2{\cdot}4H_2O$, $Ni(CH_3COO)_2{\cdot}4H_2O$, and $Zn(CH_3COO)_2{\cdot}2H_2O$, as Fe^{3+}, Y^{3+}, Co^{2+}, Ni^{2+} and Zn^{2+} raw materials, respectively [50].

Sol-gel process method had been used for the preparation of all Ferrite samples; iron nitrate was first dissolved in 50 mL of 0.2 mol/L CH_3COOH at 65 °C. To this solution, yttrium oxide dissolved in acetic acid, or cobalt acetate, or nickel acetate, or zinc acetate dissolved in 50 mL of distilled water was added and the resulting mixture was stirred for 1 h at the same temperature. In a following step, 1,2-ethanediol (2 mL) as complexing agent was added to the reaction solution. After concentrating the solutions by a rapid evaporation at 95 °C under stirring, the Y-Fe-O, Co-Fe-O, Ni-Fe-O or Zn-Fe-O nitrate-acetate-glycolate sols turned into brownish transparent gels. The oven dried (at 110 °C) precursor gel powders were ground in an agate mortar and preheated for 2 h at 800 °C in air [51].

Soft mechanic-chemical synthesis has been used to obtain powdery Nickel ferrite, $NiFe_2O_4$ in a planetary ball mill. Ni $(OH)_2$ and $Fe(OH)_3$ were used as initial compounds. This mixture was mechanically activated for 25 h, uni axial pressed and sintered at 1100 °C for 2 h [52].

Nano-crystalline Cobalt ferrites Co_x $Cu_{(1-x)}Fe_2O_4$ (x=0,0.2,0.4,0.6,0.8,1) were prepared by co-precipitation method. The desired composition was obtained by taking stoichiometric amounts of [$CoCl_2.6H_2O$], [$CuCl_2.2H_2O$] and [$FeCl_3$] and dissolved them in distilled water. The neutralization was carried out with sodium hydroxide solution. The pH of the solution was maintained at 10 and it is stirred for 2 hours. The precipitate was thoroughly washed with distilled water until they became free from impurities. The product was dried

to remove water contents. The dried powder was mixed homogeneously and is sintered at 600 °C [53].

Mahmoud has used thermal treatment method to prepare the Nickel ferrite nano-particles. Nickel nitrate and iron nitrate were used as precursors and de-ionized water as a solvent and PVP as a capping agent [54].

Upadhyay has used the sol-gel auto combustion to synthesize nano-sized Ni-Zn ferrite powder. For the synthesis of $Ni_{1-x}Zn_xFe^{2+}_zO_4$ (where x=0; 0,3; 0,5; 0,7; 1 and z= -0,025; - 0,01; 0; 0,05; 0,1; 0,15; 0,2), the method involves dissolution of metal nitrates and a complexing agent (citric acid) in distilled water and neutralization of the solution by NH_4OH. In the next step the solution was evaporated to obtain fine gel. The combustion reaction of the fine gel was initiated at 250 °C. Molar ratio of metal nitrates and citric acid was adjusted at 1:1 [55].

Nano-sized powder of magnetic manganese ferrite was prepared by co-precipitation method using manganese (II) chloride tetra hydrate, iron (III) chloride hexa-hydrate and sodium hydroxide as starting materials. The ratio between Fe (III) and Mn (II) was kept at 2:1. A 100 mL of salt solution were added drop wise to the base solution until the metallic to hydroxyl ion (M/OH) ratio became 0.2. The gray precipitates were obtained in this routine were washed and filtered repeatedly with distilled water until the pH of the residual solution reached 7. This process took about 6 to 7 h. The sample was then dried in an oven keeping temperature at 50 °C for 3 h. After attaining the powder form by motor and pestle, calcinations process was

carried out at 600 °C for 5 h to get the final product of manganese ferrite [56].

Chemical co-precipitation has been used to prepare $CoFe_2O_4$ nanostructures, it was synthesized by. A solution of 0.2 M was prepared by dissolving $Co(NO_3)_2{\cdot}6H_2O$ and $Fe(NO_3)_3{\cdot}9H_2O$ in de-ionized water. The precipitating agent was a 0.5 M NaOH solution with 100 % molar excess. Both solutions were heated separately to 65 °C and then mixed under constant stirring. The temperature was raised to 80 °C for 20 min, causing complete crystallization of the spinel phase. The precipitate was centrifuged and washed with distilled water [57].

Sol–gel technique has been used. To synthesize nano structures of $CoFe_2O_4$, $BaTiO_3Ba\ (C_2H_3O_2)_2$ was mixed with titanium (IV) n-butoxide stearic acid and glacial acetic acid at 90 °C to form a sol. The Ferro fluid was added to the sol at an adequate amount. Anhydrous 2-methoxyethanol was used to promote the gel formation. The obtained gels were dried overnight at 80 °C and sintered at 700 °C for 2 h under some conditions to prevent BTO cracking, (BTO indicate B to barium, T to titanium, O to oxide, [58].

Chapter Two

Experimental

2.1 Chemicals and Lab wares

The following materials, glassware and instruments were used for the synthesis of the targeted ferrite materials:

- Ammonium oxalate monohydrate, $(NH_4)_2C_2O_4.H_2O$, Min. assay 97 %, Prabhat Chemicals.
- Barium (II) chloride, $BaCl_2$, Min. assay 96%, Prabhat chemicals.
- Hydrochloric acid HCl, Density 1.18 g/cm^3, Min. assay 35-38 %, Loba chemie Pvt. Ltd, India.
- Cobalt (II) nitrate hexa hydrate, $Co(NO_3)_2.6H_2O$, Min. assay 98 %,CDH (industry) India.
- Cupper (II) chloride dihydrate $CuCl_2.2H_2O$, Min. assay 98 %, Scott science, UK.
- Ferrous sulphate heptahy drate $FeSO_4.7H_2O$, Min. assay 98 %, Prabhat chemicals.
- Manganese (II) sulphate, $MnSO_4$, Min. assay 98 %, Scott science, UK.

- Nickel (II) nitrate hexa hydrate, $Ni(NO_3)_2.6H_2O$, Min. assay 98%,CDH, India.
- Potassium hydroxide, KOH, Min. assay 85%, Scott science, UK.
- Potassium nitrate, KNO_3, Min. assay 87%, Scott science, UK.
- Hot plate stirrer, Bible sterling Ltd, UK. Muffle furnace. Glass wares.

2.2 Synthesis of ferrites

2.2.1 Iron ferrite, Fe_3O_4 (Fe-Fer)

A quantity of 27.8 g of $FeSO_4.7H_2O$ was dissolved in 200 mL of distilled water. Quantities of 2.0 g of KNO_3 and 15.0 g of KOH were mixed and dissolved in 100 mL distilled water in a separate beaker. Each solution was heated to about 75 °C then mixed together with vigorous stirring. A thick gelatinous green precipitate was formed. After being stirred at 90 to 100 °C for 10 min, the precipitated turns to finely divided dense black substance. The mixture was cooled to a room temperature then made acidic with little 6M HCl. The precipitate was filtered through filter paper and washed with distilled water until the wash water gave no test for sulfate with $BaCl_2$ solution. The material was dried at 110 °C for more than 1 hour and then weighed [59].

2.2.2 Nickel Ferrite (Ni-Fer)

A mixture of 12.437 g of $Ni(NO_3)_2.6H_2O$, and 13.9 g of $FeSO_4.7H_2O$ and 1 mL of 10% H_2SO_4 was dissolved in 100 mL of distilled water. A quantity of 11.0 g of $(NH_4)_2C_2O_4.H_2O$ was dissolved in 150 mL of warm distilled water. The solution was heated to about 75 °C and while stirring vigorously, the oxalate solution was taken and then added to the metal sulfate solution. The mixture was stirred while maintaining the temperature at about 90 to 95 °C for about 5 min. The yellow mixed oxalate precipitate was filtered through normal filter paper and washed with distilled water until sulfate was no longer detected in the wash (using $BaCl_2$ solution). The oxalate precipitate was dried for 2 hours at 110 °C then transferred to a porcelain crucible. The crucible was placed and calcined in a muffle at about 700 °C for 3 hours, then allowed to cool to a room temperature and weighed [59].

2.2.3 Cobalt Ferrite (Co-Fer)

A mixture of 12.441 g of $Co(NO_3)_2.6H_2O$, 13.9 g of $FeSO_4.7H_2O$ and 1 mL of 10% H_2SO_4 was dissolved in 100 mL of distilled water. A quantity of 11.0 g of $(NH_4)_2C_2O_4.H_2O$ was dissolved in 150 mL of warm distilled water. The solution was heated to about 75 °C and while stirring vigorously, the oxalate solution was added to the metal sulfate solution. The mixture was stirred while maintaining the temperature at 90 to 95 °C for about 5 min. Then the yellow mixed oxalate precipitate was filtered through normal filter paper and washed with distilled water until sulfate was no longer detected in the wash (using $BaCl_2$ solution), the mixed oxalate precipitate was dried for 2 hours at

110 °C, then transferred to a porcelain crucible and placed in a muffle at heated to about 700 °C for 3 hours. The material was allowed to cool at room temperature and then weighed [59].

2.2.4 Copper Ferrite (Cu-Fer)

A mixture of 7.597 g of $CuCl_2.2H_2O$, 13.9 g of $FeSO_4.7H_2O$ and 1 mL of 10% H_2SO_4 was dissolved in 100 mL of distilled water. A quantity of 11.0 g of $(NH_4)_2C_2O_4.H_2O$ was dissolved in 150 mL of warm distilled water. The solution was heated to about 75 °C and while stirring vigorously, the oxalate solution was added to the metal sulfate solution. The mixture was stirred while maintaining the temperature at 90 to 95 °C for about 5 min. The yellow mixed oxalate precipitate was filtered through normal filter paper and washed with water until the sulfate was no longer detected in the wash (using $BaCl_2$ solution). The oxalate precipitate was dried on the oven for 2 hours at 110 °C. The mixed oxalate precipitate was then transferred to a porcelain crucible and in a muffle and heated to about 700 °C for 3 hours. The material was allowed to cool at room temperature and weighed [59].

2.2.5 Manganese Ferrite (Mn-Fer)

A mixture of 7.217g of $MnSO_4$, 13.9 g $FeSO_4.7H_2O$ and 1 mL of 10 % H_2SO_4 was dissolved in 100 mL of distilled water. A quantity of 11.0 g of $(NH_4)_2C_2O_4.H_2O$ was dissolved in 150 mL of warm distilled water. The solution was heated to about 75 °C and while stirring vigorously, the oxalate solution was added to the metal sulfate solution. The mixture was stirred while maintaining the temperature at 90 to 95 °C for about 5 min. Then the yellow

mixed oxalate precipitate was filtered through normal filter paper and washed with water until the sulfate was no longer detected in the wash (using $BaCl_2$ solution). The oxalate precipitate was dried for several hours at 110 °C. The mixed oxalate precipitate was taken in a porcelain crucible and placed a muffle then heated to 700 °C for 2 hours. The material was allowed to cool at room temperature and weighed [59].

2.3 Characterization methods

2.3.1 Fourier Transform Infra-Red (FT-IR) spectroscopy

Fourier Transform Infra-Red (FT-IR) data of (Co-Fer), (Cu-Fer), (Ni-Fer), (Mn-Fer) and (Fe-Fer) were obtained using (Shimadzu, Japan) 8400S FT-IR spectrometer in the wave number range of 400-4000 cm^{-1}, with KBr discs. The KBr disk was prepared at weight ratio of KBr (spectral grade) to ferrite samples of about 20:1.

2.3.2 Powder X-ray Diffraction:

The powder X-ray diffraction patterns of the ferrite samples were collected from Philips PW 3719 (Voltage of 40 kV and current of 30 mA) using CuKα. (λ = 0.154 nm) radiation. The diffraction angle was scanned in the 2θ range from 10° to 70° for 2h, at a rate of 2°/ min.

2.3.3 X-Ray Fluorescence (XRF)

The powder X-ray Fluorescence spectra of the samples were collected from (Shimadzu, Japan) using ^{109}Cd as excitation source. The different elements have the characteristic X-ray peak of different wavelengths. The fluorescence intensity of each spectral line is related to the element concentration in samples. The XRF spectrometer was used to determine the elemental composition of the samples in ppm.

Chapter Three

Results and discussions

3.1 Yields of synthesized ferrites

Different ferrites were synthesized from hydrated Iron (II) sulphate and salts of transition metal cations as describe in the experimental part. These ferrites are Iron ferrite (Fe-Fer), Cobalt ferrite (Co-Fer), Copper ferrite (Cu-Fer), Nickel ferrite (Ni-Fer) and Manganese ferrite (Mn-Fer). The appearances and yields of the produced ferrites are illustrated in Table 3.1. As shown in Table 3.1, with exception of Fe-Fer, the colors of these ferrites resemble those reported in the literature. Fe-Fer characterized with dark black color which also resembles the color of commercial Fe-Fer or magnetite (Fe_3O_4). The yields percentages of these ferrites, however, were found to be different. Fe-Fer and Cu-Fer samples exhibited lower percentages of yields, whereas higher yields percentages were registered from Ni-Fer and Co-Fer. Moderate yield percentage was obtained from Mn-Fer. The obvious variation in the yields percentages could be attributed to the lack of stochiometry of reaction precursors and/or impurities associated with salts precursors. It could reasonably be due to inappropriate experimental conditions.

Table 3.1 The yields of as-synthesized ferrites

No	Samples	Appearance	%
1	Iron ferrite or Magnetite (Fe-Fer)	Black powder	40.73
2	Cobalt ferrite (Co-Fer)	Dark brown powder	52.76
3	Cupper Ferrite (Cu-Fer)	Dark violet powder	47.27
4	Nickel Ferrite (Ni-Fer)	Dark brown powder	56.84
5	Manganese Ferrite (Mn-Fer)	Black powder	51.53

3.2 X-Rays Diffraction (XRD) Analysis

Figure 3.1: The XRD pattern of the synthesized Cobalt ferrite material (Co-Fer).

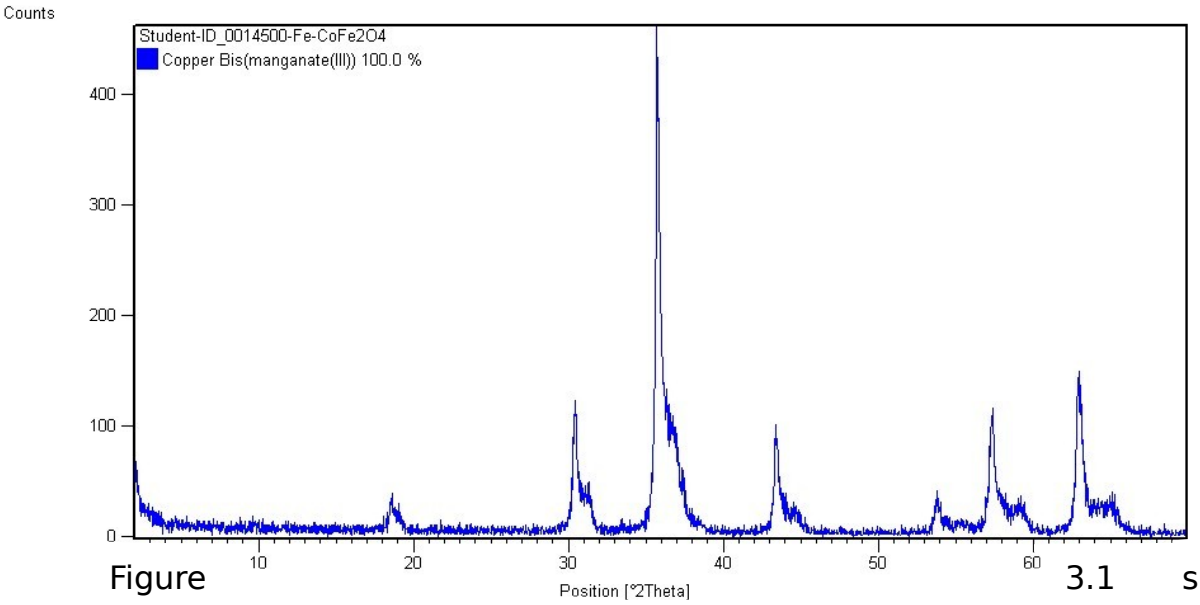

Figure 3.1 shows the diffraction peaks at 2θ angles of 18.5□, 30.2□, 35.5□, 43.0□, 53.5□, 57.0□ and 62.6□. These diffraction lines, which were marked by their corresponding

indices (111), (220), (311), (222), (400), (511) and (440), respectively, were similarly indexed to the cubic spinel structure of cobalt ferrite with nearly no impurities [60].

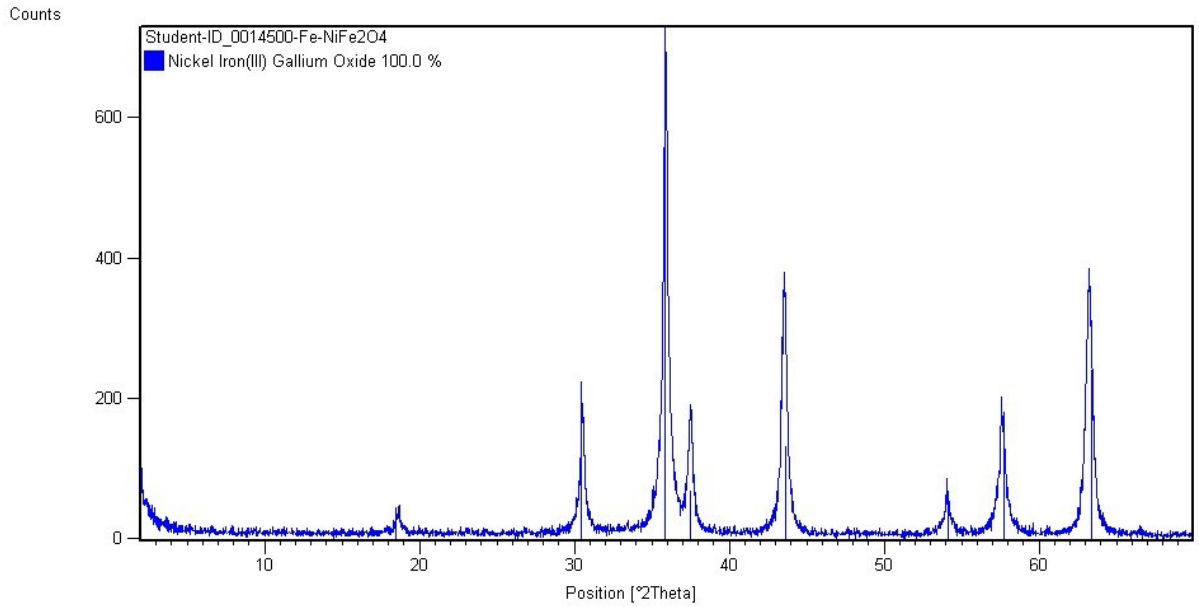

Figure 3.2: The XRD spectrum of synthesized Nickel ferrite material (Ni-Fer).

Figure 3.2 shows the diffraction peaks of the synthesized Ni-Fer are appeared at 2θ angles of 18□, 30.2□, 35.5□, 37.5□, 43.5□, 54.0□, 57.5□and 63.5□. These diffraction lines are marked by their corresponding miller indices (111), (220), (311), (222), (400), (422), (511) and (440). Interestingly, similar lines were also detected from pure nickel ferrite of cubic spinel structure as reported by Jayaprakash (2013) [61]. The presence of sharp diffraction peak at (311) was assigned to formation of bulk Ni-Fer nano particles [61].

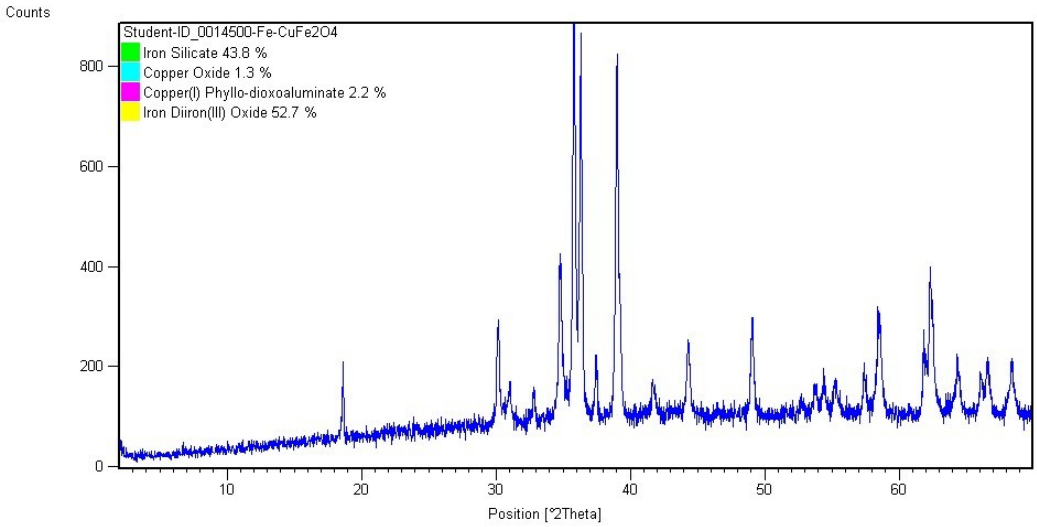

Figure 3.3: The XRD spectrum of the synthesized Cupper ferrite material (Cu-Fer).

Figure 3.3 shows the diffraction patterns of as-synthesized Cu-Fer. The peaks at 2θ angles of 18□, 30.2□, 35.5□, 39.0□, 43.5□, 49.0□, 58.0□ and 62.5□. These diffraction lines are marked by their corresponding miller indices (111), (222), (311), (400), (422), (511), (220) and (440). The synthesized Cu-Fer was found in cubic structure. The peaks with miller indices (111) and (422) did match with the standard pattern of Cu-Fer, which indicate a cubic spinel structure of copper ferrite with existence of some impurities [62].

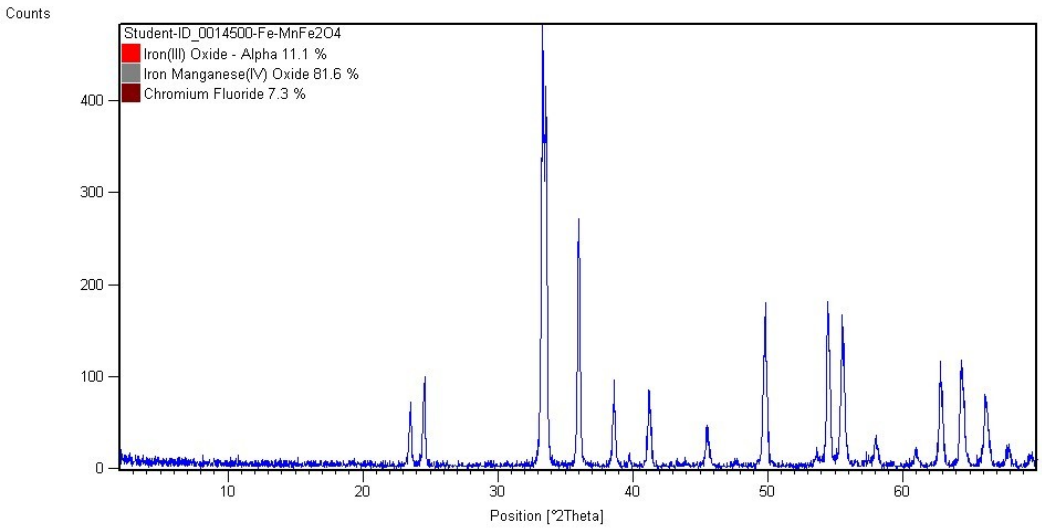

Figure 3.4: The XRD spectrum of the synthesized Manganese ferrite material (Mn-Fer).

Figure 3.4 shows the X-ray diffraction patterns of Mn-Fer ferrite. Many peaks at 2θ angles of 24.5□, 33.5□, 37.5□, 41.0□, 45.5□, 50.0□, 55.0□ and 63.5□ could be marked by their corresponding miller indices (111), (311), (220), (400), (333), (511) and (440) of the Mn-Fer. The appearance of these peaks clearly indicates the formation of the cubic spinel structure of Mn-Fer with the co-existence of some impurities [63].

3.3 Fourier Transform Infra Red (FT-IR) Analysis

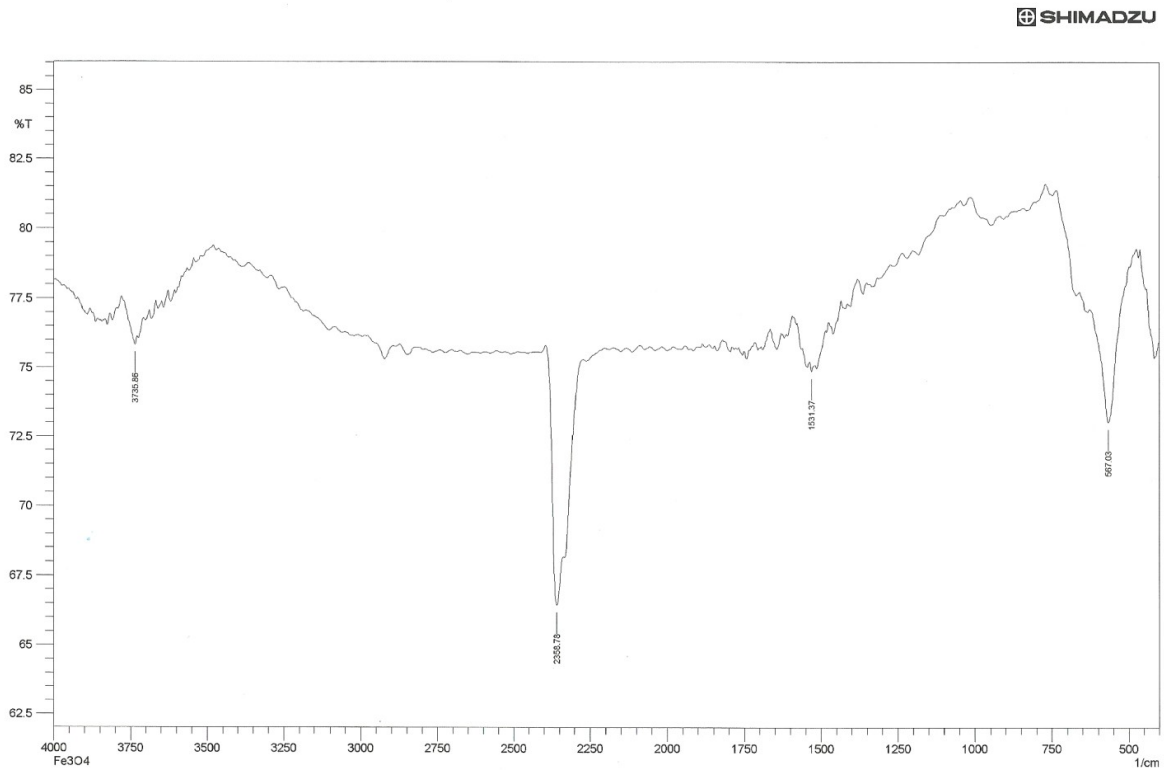

Figure 3.5: The FT-IR spectrum of synthesized Iron ferrite material (Fe-Fer)

Figure 3.5 shows the FT-IR spectrum of Fe-Fer sample (Fe_3O_4) in the range of 400 cm^{-1}-4000 cm^{-1}. The moderate band at 3736 cm^{-1} is due to O-H stretching vibration of physi-sorbed water, whereas, the peak at 1531 cm^{-1} is due to O-H bending vibration of H_2O (physi-sorbed). The peak at 2359 cm^{-1} is due to O=C=O (from adsorbed carbon dioxide), and the characteristic peak at 567 cm^{-1} corresponds to intrinsic stretching vibration of the metal (Fe-O) [64].

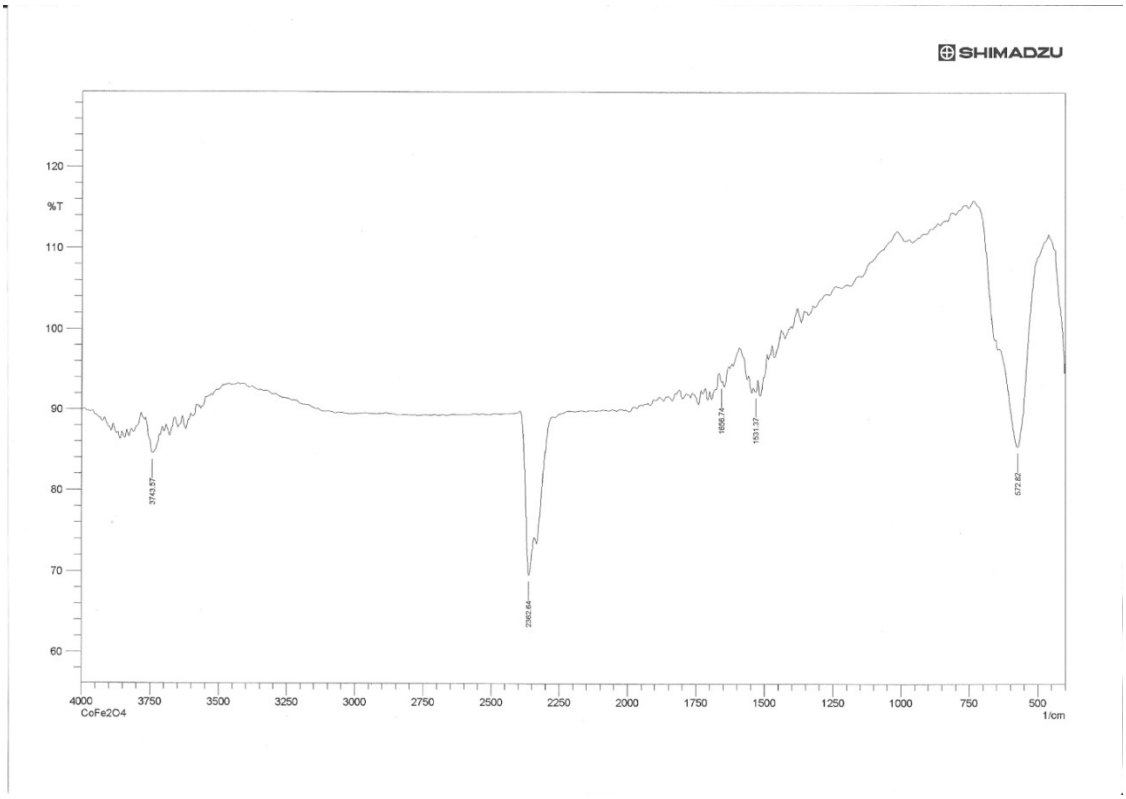

Figure 3.6: The FT-IR spectrum of synthesized Cobalt ferrite material (Co-Fer)

Figure 3.6 shows the FT-IR spectrum of sintered Co-Fer in the range 400 cm^{-1}- 4000 cm^{-1}. The moderate band at 3744 cm^{-1} is due to O-H stretching vibration of physi-sorbed water. The peak at 2363 cm^{-1} is due to O=C=O (carbon dioxide), whereas, the band at 573 cm^{-1} corresponds to intrinsic stretching vibration of the metal at the tetrahedral side Co-O. The sample contains multiple peaks (Co-O absorption bands) in the frequency region 1100-1625 cm^{-1}, which could be assigned to Co-O and Fe-O vibrations [60].

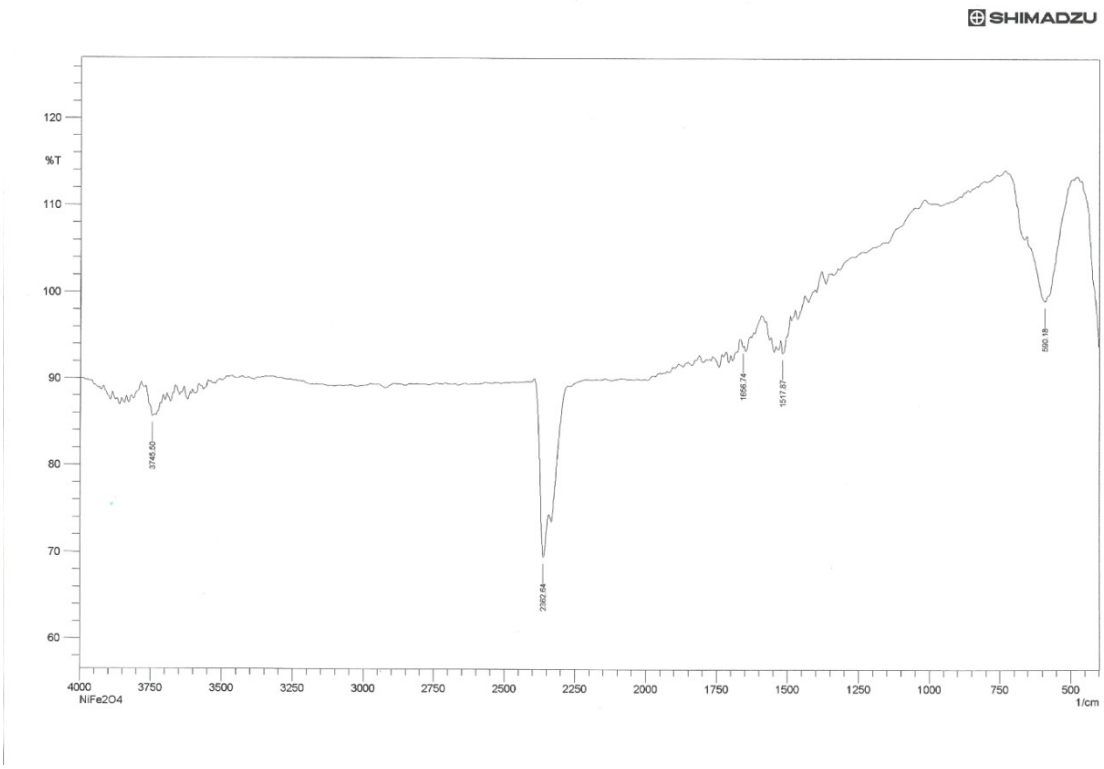

Figure 3.7: The FT-IR spectrum of synthesized Nickel ferrite material (Ni-Fer)

Figure 3.7 shows the FTIR spectrum of sintered Ni-Fer sample in the range 400 cm^{-1} - 4000 cm^{-1}. The moderate band at 3746 cm^{-1} is due to O-H stretching vibration of physi-sorbed water. The peak at 2363 cm^{-1} is attributable to O=C=O (adsorbed carbon dioxide), whereas, the band at 1518 cm^{-1} is due to O-H bending vibration of physisorbed water. The characteristic peak at 590 cm^{-1} corresponds to stretching vibration of the metal oxide at tetrahedral side structure absorption Ni_{tetra}-O [61].

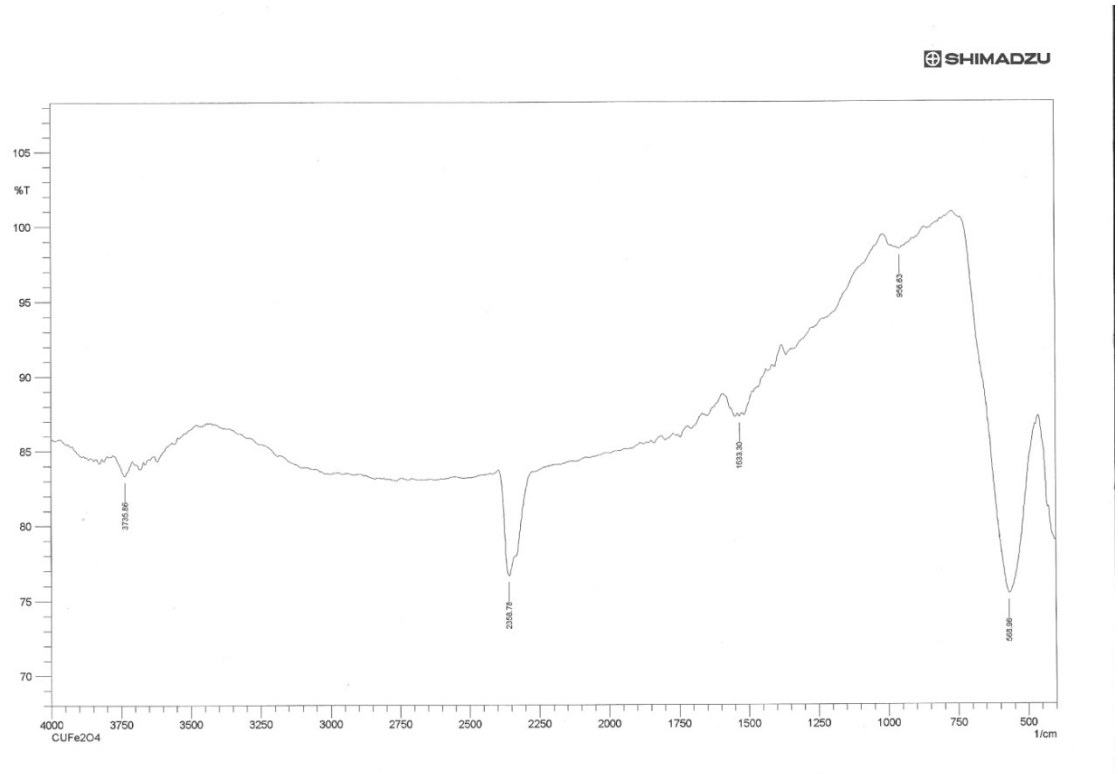

Figure 3.8: The FT-IR spectrum of synthesized Copper ferrite material (Cu-Fer)

Figure 3.8 shows the FTIR spectra analysis of sintered Cu-Fer sample in the range 400 cm^{-1}- 4000 cm^{-1}. The moderate band at 3736 cm^{-1} are appear due to O-H stretching vibration, were the peak at 1518 cm^{-1} due to O-H bending (this two peak appear from moiser of out surface), the peak at 2359 cm^{-1} are due to O=C=O (carbon dioxide which produced from burning of compound), and the characteristic peak at 569 cm^{-1} corresponds to intrinsic stretching vibration of the metal at the tetrahedral side M_{tetra}-O ,usually absorbed in the range 450 -500 cm^{-1} assigned to octahedral metal stretching [M_{octa}-O] [62].

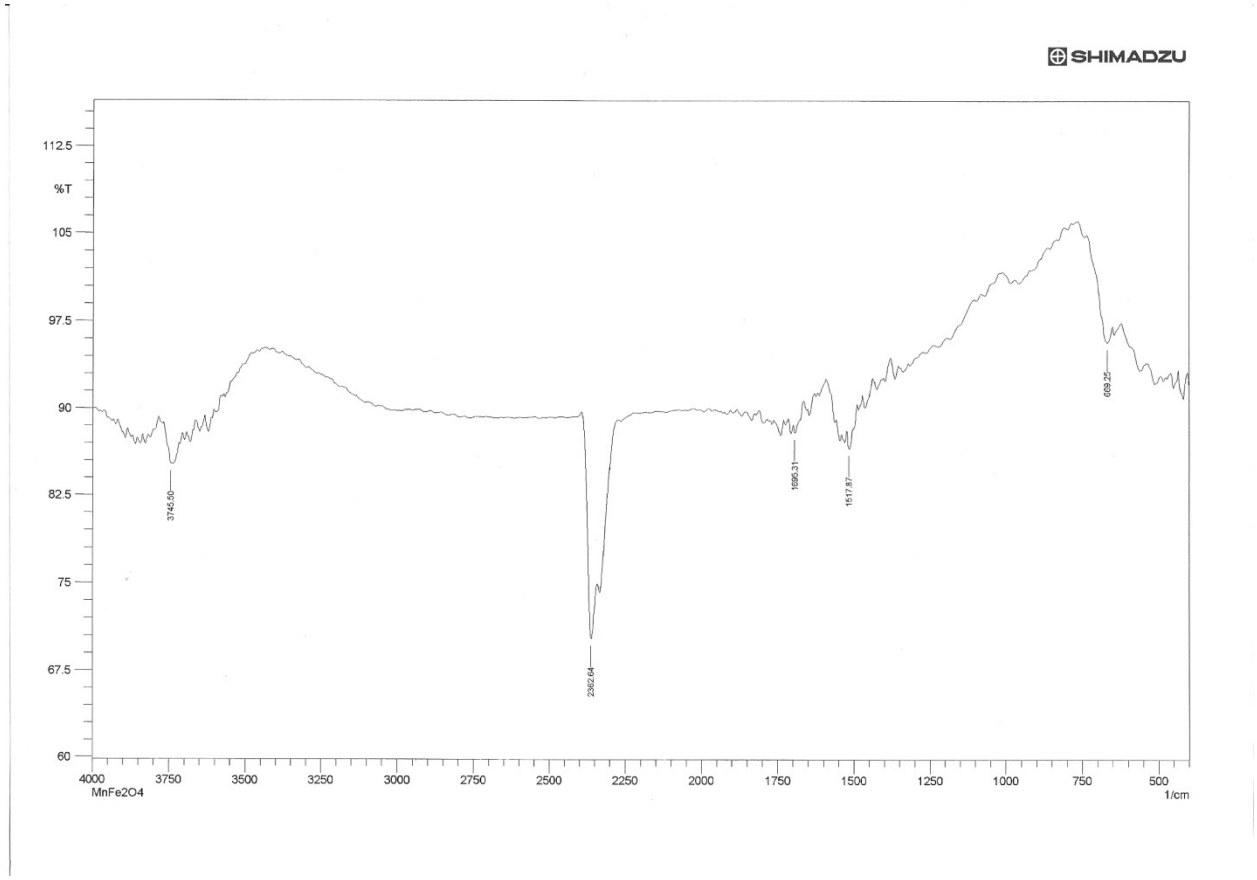

Figure 3.9: The FT-IR spectrum of synthesized Manganese ferrite material (Mn-Fer)

Figure 3.9 shows the FTIR spectrum analysis of sintered Mn-Fer sample in the range 400 cm^{-1}- 4000 cm^{-1}.The moderate band at 3746 cm^{-1} is due to O-H stretching vibration, whereas the peak at 1518 cm^{-1} is due to O-H bending (from physi-sorbed water). The peak at 2363 cm^{-1} is assigned to O=C=O, and the characteristic peak at 669 cm^{-1} corresponds to stretching vibration of the metal at the tetrahedral side [Mn-O] [63].

3.4 X-Ray Fluorescence (XRF) Analysis

Table 3.2: X Ray Fluorescence analysis data and expected empirical formulas

Sample	Fe	Co	Cu	Ni	Mn	Empirical Formula (Calculated)	Empirical Formula (Theoretical)
Co-Fer	34.59	31.99	-	-	-	$Co_{1.2}Fe_{1.8}O_{3.2}$	$CoFe_2O_4$
Cu-Fer	35.76	-	58.31	-	-	$Cu_2Fe_{1.5}O$	$CuFe_2O_4$
Ni-Fer	48.76	-	-	42.60	-	$Ni_{1.8}Fe_2\ O_{1.2}$	$NiFe_2O_4$
Mn-Fer	53.54	-	-	-	36.93	$Mn_{1.5}Fe_{1.8}O_2$	$MnFe_2O_4$
Fe-Fer	91.67	-	-	-	-	Fe_4O_2	Fe_3O_4

Table 3.2 shows the XRF analysis results of all ferrite samples. For Fe-Fer sample the practical (calculated from XRF analysis) percentages of Fe^{3+} and O^{2-} (weight difference) were found to be 91.67 %, and 8.33 %, respectively. Hence by calculating the number of moles for any element, an empirical formula of Fe_4O_2 is obtained, which is not resemble the theoretical formula Fe_3O_4 for iron ferrite (magnetite).

For Co-Fer sample, the practical percentages of Co^{2+}, Fe^{3+} (calculated from XRF analysis) and O^{2-} (calculated by weight difference) were found to be 31.99 %, 34.59 % and 33.42 %, respectively. Hence by calculating the number of moles for any element, the empirical formula $Co_{1.2}Fe_{1.8}O_{3.2}$ is obtained, which is quite closed to the theoretical formula $CoFe_2O_4$ for spinel ferrite.

For Cu-Fer, Ni-Fer, Mn-Fer samples the practical percentages of Cu^{2+}, $Ni^{2+,}$ $Mn^{2+,}$ Fe^{3+} and O^{2-} (weight difference) were found to be 58.31 % , 42.60 %, 36.93 %, 35.76 % and 6.02 %, respectively. Hence by calculating the number of moles for any element, the respective empirical formulas $Cu_2Fe_{1.5}O$, $Ni_{1.8}Fe_2O_{1.2}$ and $Mn_{1.5}Fe_{1.8}O_2$ are obtained, which do not resemble the respective theoretical formulas $CuFe_2O_4$, $NiFe_2O_4$ and $MnFe_2O_4$ for spinel ferrites. These variations in the percentages of synthesized ferrite samples could be related to impure precursor salts which were used in the synthesis of the materials. They could contain undetected impurities which interfere and hence spoiled the stochiometry of the reaction. Human errors from the operator of XRF instrument, which was used to detect the targeted metals, could have also some influences in the accuracy of the results. Further studies on this are really demanded, such as conducting analysis using different XRF spectrometer or using different spectroscopic technique, for instance AAS.

Chapter Four

Conclusions

Ferrite of Ni(II), Co(II), Cu(II), Mn(II), Cu(II) and Fe(II) were synthesized under normal conditions by adopting a co-precipitation method using simple salts of these divalent metal ions. The synthesized ferrite materials were labeled as Nickel ferrite (Ni-Fer), Cobalt ferrite (Co-Fer), Manganese ferrite (Mn-Fer), Copper ferrite (Cu-Fer), and Iron ferrite (Fe-Fer), respectively. These were found to exhibit some variations in their appearances whereas their yields were observed to be close. The produced ferrites were characterized with many spectroscopic techniques. The FT-IR results of the samples showed the existence of both Fe-O and M-O bands; whereas XRD diffraction data emphasized the presence of diffraction lines of the spinel type MFe_2O_4 (M=Co, Ni, Cu, Mn or Fe) ferrites. The empirical formulas of these ferrites were calculated from the XRF elemental analytical results, but showed

obvious variations from theoretical formulas. The variations in the percentages of synthesized ferrite samples were related to impurities associated with salts precursors as well as human errors from the operators of XRF instrument. The doubt on these variations would be released, if proper lab facilities, pure chemicals and appropriate reaction conditions were offered for the preparation of these ferrites.

References

[1] Cullity, B. D., (1972). Effect of magnetic field applied during secondary annealing on texture and grain size of silicon steel. *Script material.* 48, 1343-1347.

[2] Barbers, V. A., (1995). Solid state synthesis of α-Fe and iron carbide nano particle by thermal treatment of amorphous Fe_2O_3. *Hand Book of Magnetic Materials.*, 8, 189.

[3] Costa, R. C., (2006). Mn–Zn nano-crystalline ferrites synthesized from spent Zn–C batteries using novel gelatin method. *J. Hazard. chem. Center ., 6 ,* 129 -171.

[4] Goldman, A., (1990). Modern Ferrite Technology. Van Nostrand, Reinhold, New York.

[5] Chen, C. W., (1990). Magnetism and Metallurgy of Soft Magnetic Materials, North-Holland, Amsterdam.

[6] Bosch, R. G., (1977). Microstructure of hard ferrite and their magnetic properties. *Journal dephysique*. 1, 69-72.

[7] Perez, O. P., Sasaki. H., (2002). Synthesis and magnetic properties of cobalt ferrite with different morphology. *National institute of technology Rourkela*. *Appl. Phys.,* 91, 6958–6960.

[8] Nanba, N., Kobayashi, S., (1978). Semi conductive Properties and cation Distribution of Copper Ferrites $Cu_{1-\delta}Fe_{2+\delta}O_4$. *Japanese Journal of Applied Physics*, 17, 1819-1823.

[9] Sawant, S. R., Patil, R. N., (2010). Magnetic Hysteresis Studies on Slow Cooled and Quenched CuxZn1−xFe_2O_4 Sys-tem. *Solid State Communications*, 40, 1981, 391-394.

[10] Park, I. W., Yoon, M., (2003). Magnetic Properties and Microstructure of Cobalt Nano particles in a Polymer Film. *Solid State Communications*, 126, 7, 385-389.

[11] Richa, S., Yadav, B. C., (2012). Ferrite Materials: Introduction, Synthesis Techniques, and Applications as Sensors, *International Journal of Green Nanotechnology*, 4, 141–154.

[12] Mallik, R. K., (2012). Synthesis and magnetic properties of cobalt ferrite with different morphology, *national institute of technology*.

[13] Goldman, A., (1993). Modern Ferrite Technology, Marcel Dekker, New York.

[14] Lu, J., S, Maa., Sun, J., Xia, C., Liu, C., Wang, Z., Zhao, X., Gao, F., Gong, Q., Song, B., Shuai, X., Ai, H., Gu, Z., (2009). *Biomaterials*. 30, 2919.

[15] Tromsdorf, U. I., Bigall, N. C., Kaul, M., Bruns,G. O., Nikolic, T., Mollwitz, M. S., Sperling, B. R., Reimer, A., Hohenberg, R., Parak, H., Forster, W. J., Beisiegel, S. U., Adam, G., Weller, H., (2007). Preparation and characterization of spindle-like Fe_3O_4 mesoporous nano paricle. *Nano Lett*., 7, 2422.

[16] Boni, A., Marinone, M., Innocenti, C., Sangregorio, C., Corti, M., Lascialfari, A. M., Mariani, F., Orsini, G. P., Casula, M. F., (2008). Magnetic and relaxometric of Manganese ferrite .*J. Phys. D: Appl. Phys*., 41- 134021.

[17] Teja, A. S., Koh, P. Y., Prog, C., Growth, C. M., (2009). Comparison of surface effects in SiO_2coated and uncoated nickel ferrite nano particles, *journal of homepage*., 55, 22–45.

[18] Smit, J. H., Wijn, P. J., (1959). Ferrites-Physical Properties of Ferromagnetic Oxides in Relation to their Technical Applications. Wiley, New York, NY.

[19] Yang, L., Xie, Y., Zhao, H., Wu, X., Wang, Y., (2005). Comparison of surface effects in SiO_2coated and uncoated nickel ferrite nano particles , *journal of homepage*., 49, 1029– 1033.

[20] Shimada, T., Tachibana, T., Nakagawa, T., Yamamoto, T. A., (2004). Comparison of surface effects in SiO_2 coated and uncoated nickel ferrite nano particles. *J. Alloys Comp.,* 379, 122–126.

[21] Villette, C., Tailhades, P., Rousset, A., (1995). Structure and Magnetic Properties of nano crystalline Copper Ferrite Synthesis by Sol-gel Auto combustion Method. *J. Solid state Chem.*, 117-64.

[22] Hench, L. L., West, J. K., (1990). Principles of Electronic Ceramics, John Wiley & Sons.

[23] Van, A., Groenou, B., Bongers, P. F., Stuijts, A. L.,(2007). Magnetic and transport properties of Co-doped Fe_3O_4 films. *Materials Science and Engineering*. 3 , 1968-69, 317.

[24] Heck, C., (1974). Magnetic Materials and their Applications, Butterworth's, London.

[25] Smit, J. H., Wijn, P. J., (1959). Di electric of cobalt substituted M-type barium hexa ferrite prepared by co-preciptation.*j mater sci:mater eledtron* ,18, 527-534.

[26] Alex, G., (2010). Modern Ferrite Technology, 2nd Edition.vol25 mb .p 229.

[27] Stuijts, A., Rathenau, L. G., Weber, G. H., (1964). Introduction of magnetic material, *American ceramic society symposium* , 16-141.

[28] Moulson, A. J., Herbert, J. M., (1990). Electro ceramics Materials Properties Applications, 1st Edition, Chapman & Hall, London.

[29] Bragg, W. H., Phil, M., (1915). X Rays and Crystal Structure Data of Inorganic Compounds. Landolt. vol, 30- 305.

[30] Clarricoats, B., Barlow, H. M., (2012). Characterization and electromagnetic studies on NiZn and NiCuZn ferrites prepared by microwave sintering technique. *Material science and application* .3. 628-632.

[31] Horovitz, K. L., Johnson, V. A., (1959). Solid State Physics, Academic Press, New York and London, 6.

[32] Sawataky, G. A., Morrish, A.H., (1996). Structure and magnetic properties of zinc and aluminum– substituent cobalt ferrite prepared by co-precipitation method. *J. Appl. Phys*. 39. 12- 14.

[33] Dormann, J. L., Nogues, M., (1990). Synthesis and magnetic properties of manganese ferrite. *J. Phys. Condense. Matter*. 2, 1223 .

[34] Deraz, N. M., Alarifi, A., (2012). Micro structure and magnetic Studies of zinc ferrite nano particle. *J, Anal. Appl. Pyrolysis*. 94 - 41.

[35] Coey, D., (2009). Magnetism and Magnetic Materials‖ Published in the United States of America by Cambridge University Press, New York.

[36] Verway, E. J., Haayman, P. W., Romejn, F, C., (1994). Magnetic Studies of zinc ferrite nano particle *. J. Chem. Phys*. 151- 181.

[37] Pillai, S. O., (2008). Synthesis and characterization of Nickel supestituted Aluminum ferrite. *J . Alloys Compd*. 50, 13- 17 .

[38] Deraz, N., Alarifi, M. A., (2012). Micro structure and magnetic Studies of zinc ferrite nano particle. *J, Anal. Appl. Pyrolysis*. 94 - 41.

[39] Azha, S. G., (2013). Synthesis and Characterization of nano-crystalline $Ni_{(0.6)}$ $Zn_{(0.4)}$ Fe_2O_4 Spinel Ferrite Magnetic, *Material Physics Procedia.,* 49 , 44 – 48.

[40] Wohlfarth, E. P., (1980). Preparation and characterization of nano Mn –Zn ferrite . *Journal of magnetism and magnetic materials. 202(1),77-84.*

[41] Vaidyanathan, G., (2008). Effect of zinc substitution on structure and magnetic properties of cobalt ferrite. *Indian Journal of Engineering and Material Science*, 11, 289-294.

[42] Sarangi, P. P., (2010). Synthesis and characterization of pure single phase Ni–Zn ferrite nano powders by oxalate based precursor method. *Journal home page Powder Technology* 203, 348–353.

[43] Patil, K.C., Sudar, S. Manoharan, G. D.,(eds. Nicholas P. Cheremisin off, Marcel Dekker, INC, New York .Handbook of Ceramics and Composites., 1, 469.

[44] Hassadee, A., (2011). Effect of zinc substitution on structural and magnetic properties of cobalt ferrite. *Procedia Engineering* 32, 597 – 602.

[45] Auzans, E., Zins, D., Massart, R., (1999). Temperature and magnetic resonance of Zn-Mn Gadolinium, gold, iron magnetic nano particles and cytoine synergy in hyperthermia. Science 34, 1253- 54.

[46] Rozman, M., Drofenic, M., (1995). Synthesis of Co-,Co-Zn and Ni-Zn ferrite powder by the microwave-hydrothermal method. *Ceram, Soc*. 78 - 2249.

[47] Thakur, A., (2003). Study of electrical and dielectric properties of In^{3+} substituted Mg-Mn ferrite synthesis by citrate precursor method. *International journal of theoretical and applied science.*1(1). 1-7.

[48] Makovec, D., Kosak, A., (2004). Study of Magnetic properties of Mn-Zn ferrite synthesis by glycine-nitrate auto-combustion process. *Advanced materials research Nanotechnology.* 15, 1-60.

[49] Shunli, H., (2006). Preparation and properties of nano size Mn-Zn ferrite from δ FeOOH. *Science direct* .25(6), 466-470.

[50,51] Aurelija, G., Darius, J., Aldona, B., Aivaras, K., (2010). Sol-Gel Synthesis and Characterization of Selected Transition Metal nano-Ferrites. *Material Science ISSN* 1392– 1320. 17, no 3.

[52] Ravindranathan, P., Patil, K. C., (2005). Effect of firing temperature on microstructure and magnetic properties of nano crystalline $NiZnFe_2O_4$ prepared by weight and dry method. *Journal of analytical and applied pyrolysis*, 66, 688- 692.

[53] Balavijayalakshmia, J., Suriyanarayananb, N., Jayaprakashc, R., Gopalakrishnanc, V. (2013). Effect of concentration on dielectric properties of Co-Cu ferrite nano particles. *Physics Procedia* 49 , 49 – 57

[54] Naseri, M., Goodarz, B. E., Saion, A. H., Abbastabar, H. M., Shaari, A. H., (2011). Simple preparation and characterization of Nickel ferrite. *Powder Technology*, 151(14), 1031- 1035.

[55] Chandan, U., Verma, H. C., Anand, S., (2004). The structure and magnetic properties of $Zn_{1-x}Ni_xFe_2O_4$ ferrite nano particles prepared by sol–gel auto-combustion, *J Appl. Phys*. 95, 1015.

[56] Elahi, I., Zahira, R., Mehmood, K., Jamil, A., Amin, N., (2012). Co-precipitation synthesis, physical and magnetic properties of manganese ferrite powder, *African Journal of Pure and Applied Chemistry*, 6, (1), 1- 5.

[57] Mousa, I., Oleiwi, O., Resul, Y., Abdullah, N., (2012). Effect of chromium addition on the structural, morphological and magnetic properties of nano-crystalline cobalt ferrite system. *Ceramic international* 38, 6671-6676

[58] Flores, V., Corral, B., Bueno, D., Ziolo, R. F., (2010). Synthesis and Characterization of Sodium Potassium Niobate ($Na_{0.5}K_{0.5}NbO_3$)–Nickel-Zinc Ferrite ($Ni_{0.6}Zn_{0.4}Fe_2O_4$) Composite, *Acta Materialia.*, 58, (3), 764- 769.

[59] Jolly, L.W., (1991). The synthesis and characterization of Inorganic compounds. *Waveland and App*. Vol , 524- 525. press Inc., USA

[60] Koseoglu[a], Y., (2012). Effect of chromium addition on the structural, morphological and magnetic properties of nano-crystalline cobalt ferrite system, *ceramics international,* 38, 3625-3634.

[61] Jayaprakash, R., (2013). Synthesis and Characterization of nano crystalline $Ni_{(0.6)}$ $Zn_{(0.4)}$ Fe_2O_4 Spinel Ferrite Magnetic Material, *Physics Procedia* 49, 44 – 48.

[62] Balavi, J., (2013). Effect of concentration on dielectric properties of Co-Cu Ferrite nano-particles. *J. Physics Procedia*. 49, 49 – 57.

[63] Chang, Y., (2011). Relativities of hydrogen protons in aqueous solution of gold-coated manganese ferrite nano-particles. *Journal of the Korean physical society*, 62, 11, june 20B, 1696-1701.

[64] Williams, H. D., (1935). Spectroscopic method in organic chemistry, 3rd edition, fellow of Churchill College, Cambridge.

[65] Hennery, S. W., William, B., X-ray Diffraction (XRD), United Kingdom London University. *Royal society*. 65 (2). 163- 182.

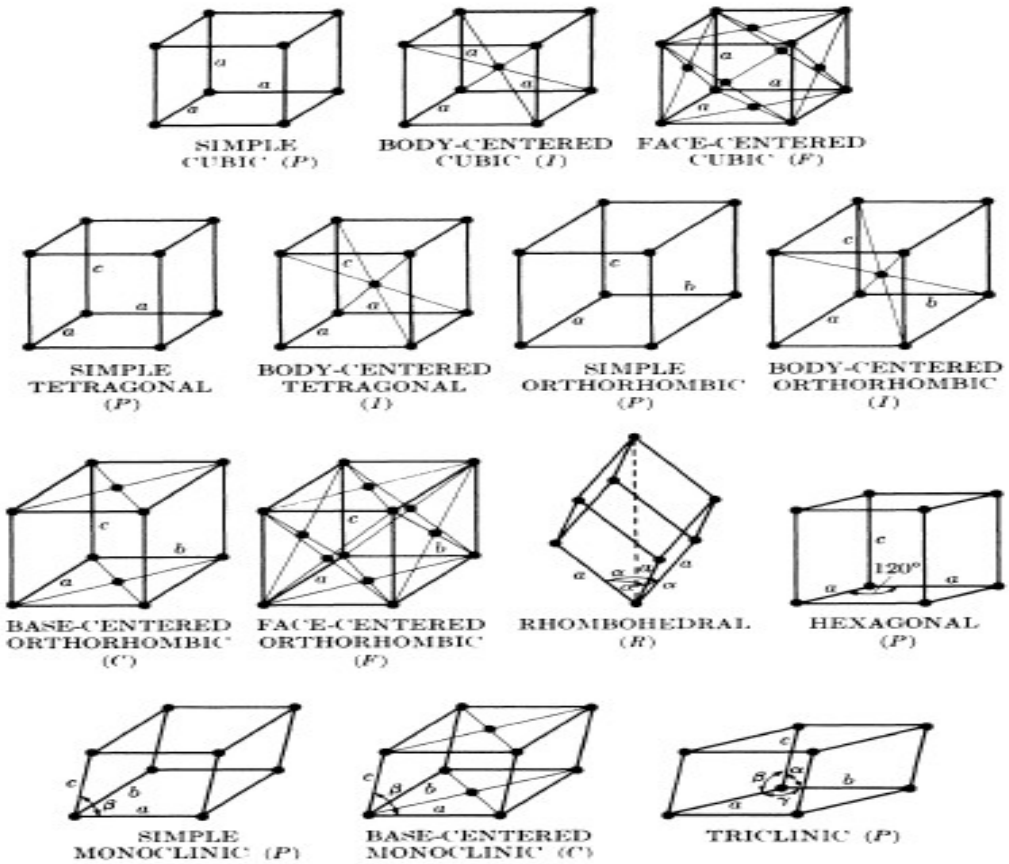

Appendices

A.1. The Geometry of crystals [65].

B.1. Crustal classes and their axis system [65].

Crystal class	Axis system
Cubic	$\boldsymbol{a} = \boldsymbol{b} = \boldsymbol{c},\ \alpha = \beta = \gamma = 90^\circ$
Tetragonal	$\boldsymbol{a} = \boldsymbol{b} \neq \boldsymbol{c},\ \alpha = \beta = \gamma = 90^\circ$
Hexagonal	$\boldsymbol{a} = \boldsymbol{b} \neq \boldsymbol{c},\ \alpha = \beta = 90^\circ,\ \gamma = 120^\circ$
Rhombohedral	$\boldsymbol{a} = \boldsymbol{b} = \boldsymbol{c},\ \alpha = \beta = \gamma \neq 90^\circ$
Orthorhombic	$\boldsymbol{a} \neq \boldsymbol{b} \neq \boldsymbol{c},\ \alpha = \beta = \gamma = 90^\circ$
Monoclinic	$\boldsymbol{a} \neq \boldsymbol{b} \neq \boldsymbol{c},\ \alpha = \gamma = 90^\circ,\ \beta \neq 90^\circ$
Triclinic	$\boldsymbol{a} \neq \boldsymbol{b} \neq \boldsymbol{c},\ \alpha \neq \beta \neq \gamma \neq 90^\circ$

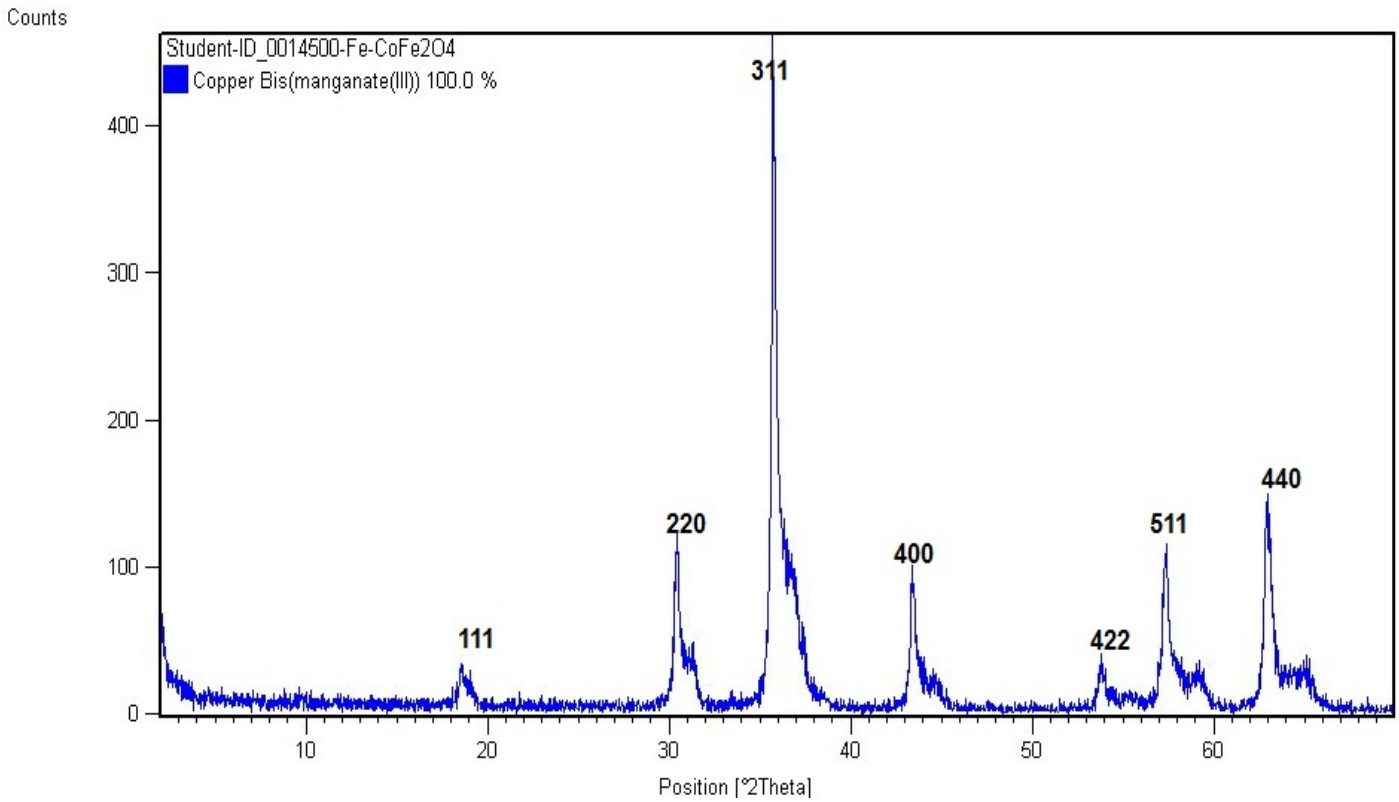

C.1: XRD diffraction lines of Co-Fer with miller index.

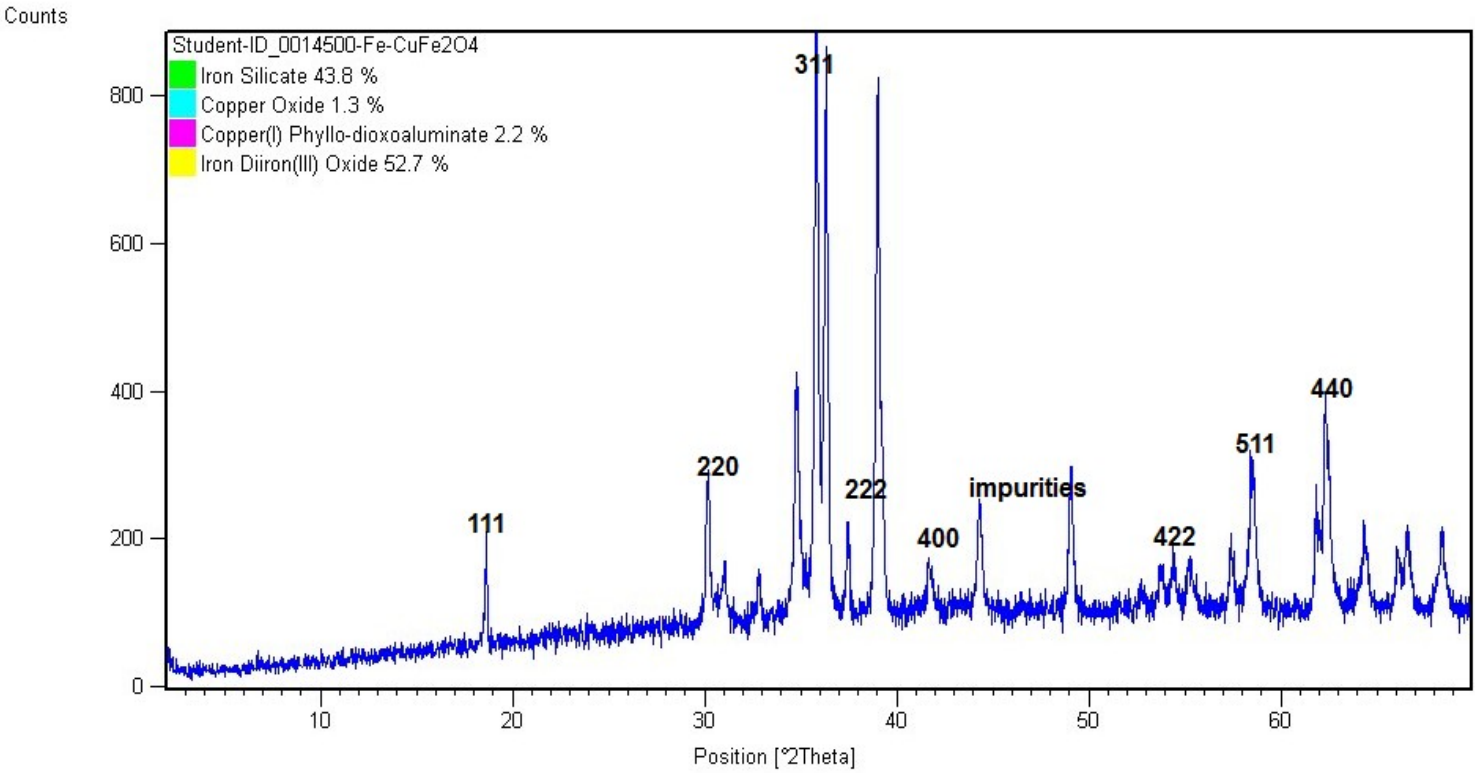

C.2. XRD diffraction lines of Cu-Fer with miller index.

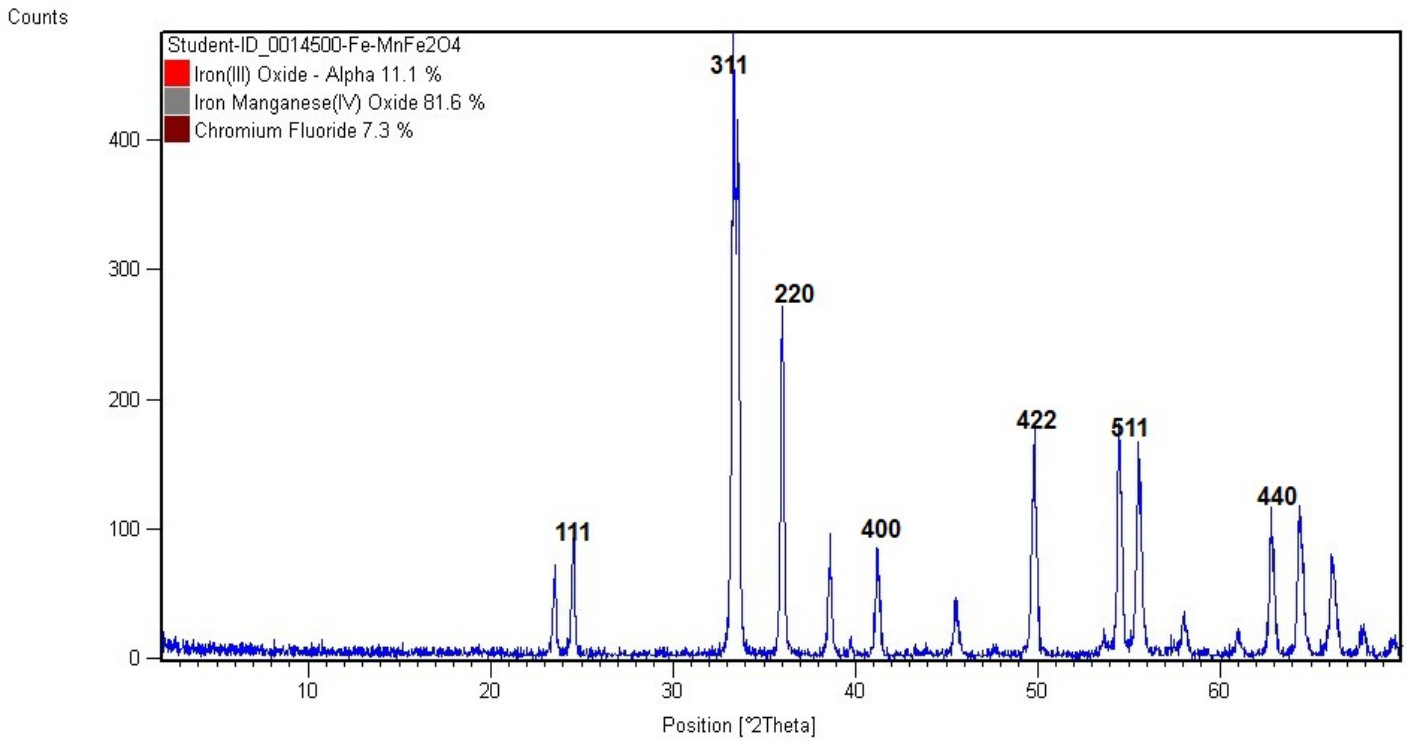

C.3. XRD diffraction lines of Mn-Fer with miller index.

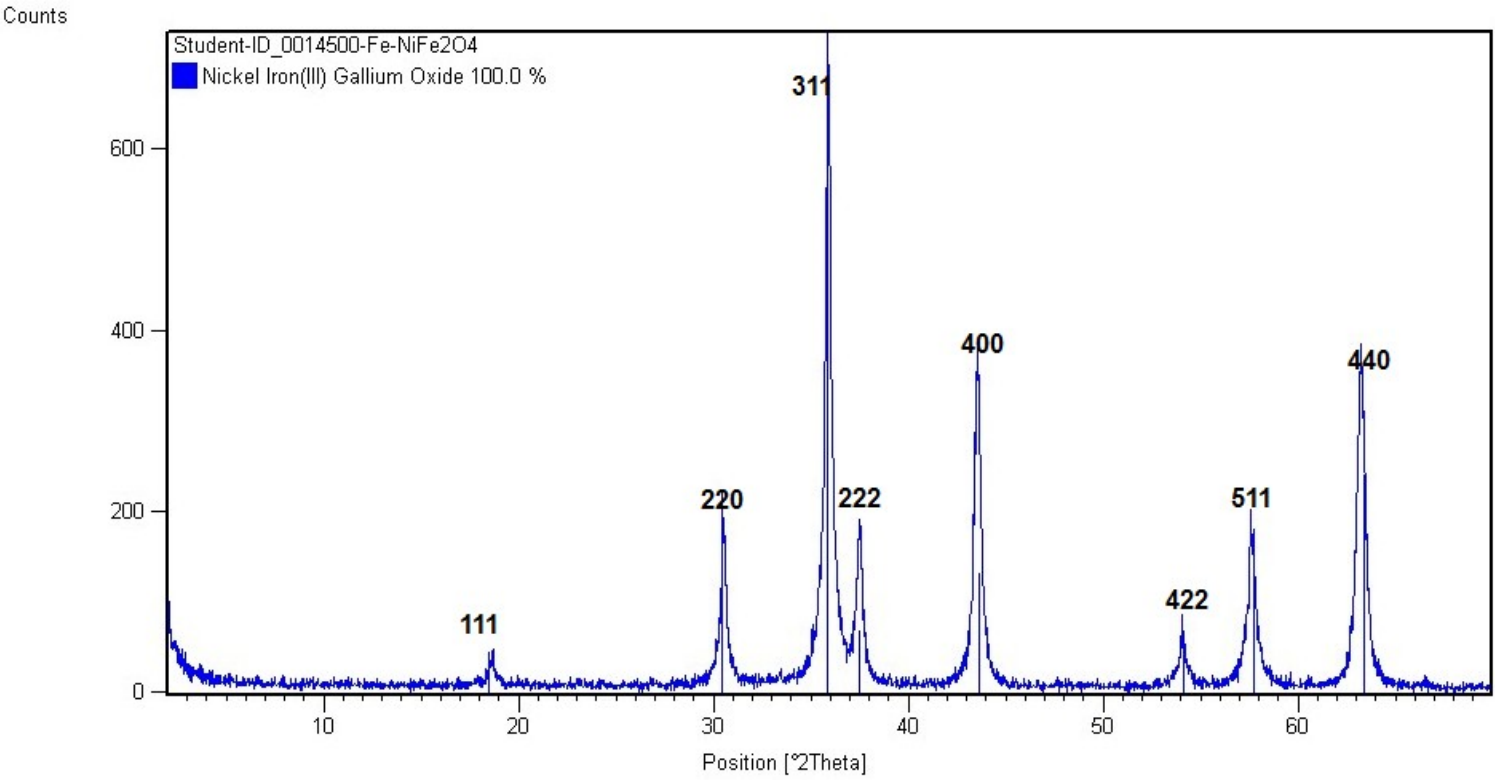

C.4. XRD diffraction lines of Ni-Fer with miller index.